

(Invited) Wave-Matter Interactions at the Chip Scale: Devices, Systems and Opportunities

Ruonan Han

Massachusetts Institute of Technology, Cambridge, MA

Abstract—In this paper, we review the recent progress on microelectronic devices and systems, which utilize different modalities of wave-matter interactions for emerging applications. Targeting at the rotational modes of gas molecules in low-THz regime, a dual-frequency-comb spectrometer in CMOS is presented, which leverages high parallelism in ultra-broadband spectral sensing. Wide molecular identification range and absolute specificity are demonstrated. Next, based on the same principle, a CMOS molecular clock is built, which references its 80-MHz output to a 231.061-GHz transition line of carbonyl sulfide molecules. The clock delivers a long-term frequency instability at 10^{-10} level, and potentially at 10^{-11} and below in the future. The vibrational modes of large bio-molecules possess great potentials in medical diagnosis, signal generation in the mid-THz range is required. To this end, a SiGe radiator array which delivers a record total radiated power of 0.1 mW at 1 THz is shown. Lastly, the paper reviews a CMOS magnetometer work, which is based on electronic spin resonance of nitrogen-vacancy centers in diamond. This is the first demonstration of CMOS-integrated quantum sensing.

Index Terms—rotational-vibrational spectroscopy, molecular clock, terahertz, magnetometry, quantum sensing, CMOS

I. INTRODUCTION

Across the entire electromagnetic (EM) spectrum, various modalities of interaction between EM waves and microscopic particles (molecules, atoms and electrons) exist. Some examples are illustrated in Fig. 1. Although the physics of all these interactions have been well studied, the extent of them being utilized in practical applications varies significantly. For instance, medical imaging using nuclear magnetic resonance in radio/microwave frequency has been a common practice; and electronic transition in optical frequency has already been the enabler for all lasers, photodiodes, etc. In comparison, the wave-matter interactions at the spectrum between microwave waves and infrared, namely the terahertz (THz) band, remains relatively unexplored. Given the limited accessibility of THz hardware, so far THz spectroscopy probing the rotational and vibration modes of gas molecules is only adopted in astronomy for the analysis of interstellar dust.

There are emerging opportunities when we conduct wave-matter interactions, from RF to optical frequencies, with highly-affordable hardware and at a very small scale—ideally in close proximity to a CMOS chip. In this paper, a few silicon-chip prototypes aligning with such a road map are reviewed. They include a signal source and broadband microsystem for THz rotational/vibrational spectroscopy [1]–[3], a chip-scale molecular clock [4], [5] and room-temperature quantum magnetometer [6]. These efforts have enabled significant sensing capabilities, and are expected

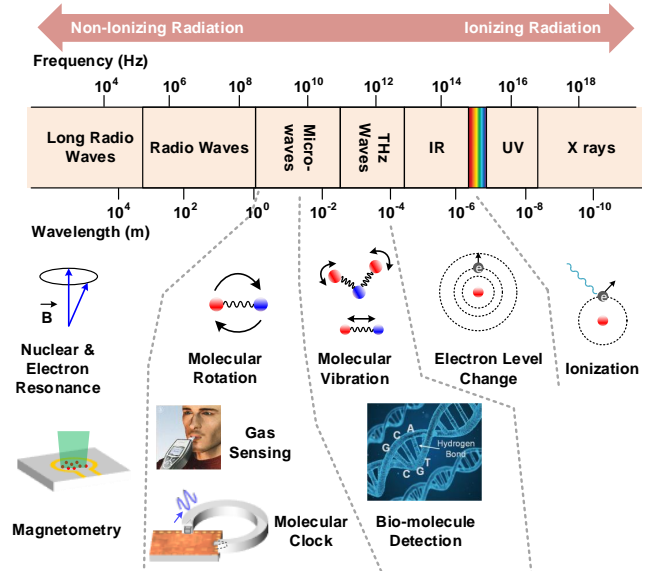


Fig. 1: Wave-matter interaction across the EM spectrum.

to open up new application spaces related to molecular identification, time-keeping, bio-chemical analysis, advanced medical research, and so on.

II. ROTATIONAL-VIBRATIONAL THZ SPECTROMETER: DUAL-COMB GAS SENSOR AND 1-THZ RADIATOR ARRAY

Rotational modes of polar molecules, when excited by a THz wave, lead to sharp absorption lines in a spectroscopic system. At low-pressure (<10 Pa), the Doppler-limited linewidth is below megahertz (i.e. $Q=10^5\sim 10^6$), enabling “absolute specificity” for gas sensing. With a 100-GHz tuning range, almost all polar molecules heavier than hydrogen cyanide can be detected [2]. Although the recent progress in THz CMOS circuits has fully shown the feasibility of a low-THz (~ 0.3 THz) transceiver in CMOS, the aforementioned bandwidth remains a big challenge, as all THz circuits rely on high- Q resonance for efficient operations. To address such performance tradeoff, we introduced a dual-frequency-comb architecture, which divide the 220-to-320-GHz band into 20 equally-spaced sub-channels and scan them in parallel with 20 transceivers located on two identical chips using 65-nm CMOS technology (Fig. 2(a)) [1]. Since now each transceiver only needs to cover 5-GHz bandwidth, positive feedback is introduced in the THz front-ends to maximize the activity of transistors (hence high efficiency across the entire 100-GHz band). One

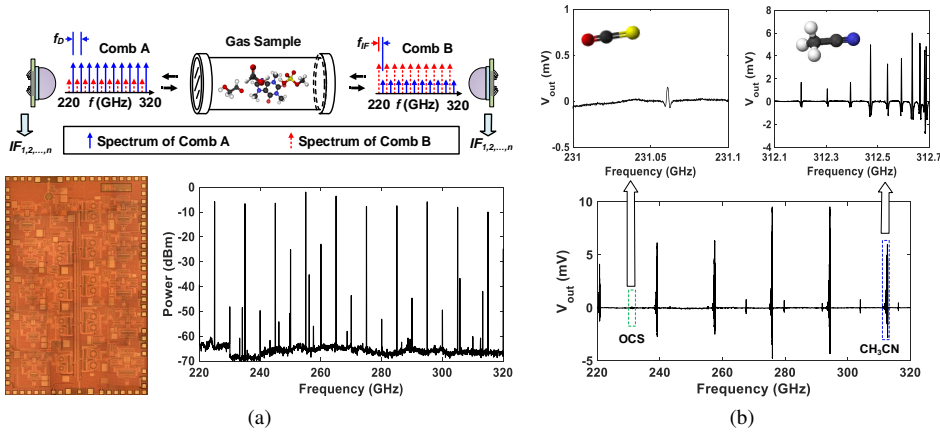


Fig. 2: Dual-THz-comb spectrometer for gas sensing [1], [2]: (a) micrograph of the CMOS die and measured output comb spectrum. (b) Measured absorption spectrum of a gas mixture sample with carbonyl sulfide (OCS) and acetonitrile (CH₃CN) ($V_{OCS}:V_{CH_3CN} \approx 1:60$).

critical challenge associated with the high-parallelism scheme is the need for very compact THz circuit structures, in order to accommodate as many as 10 transceivers on a die. To this end, EM circuit structures with high versatility and simultaneous THz transmission and reception are adopted [7]. Consuming 1.7-W DC power, the spectrometer chip has 5.3 mW of total radiated power and 15~20 dB of sensing noise figure [1]. In a gas-sensing demonstration, the chip is able to capture all spectral features of molecules inside a gas mixture (Fig. 2(b)) with a characterized sensitivity at *ppm* level [2]. A standard pre-concentration of the gas should enhance the sensitivity to sub-*ppb* level. Terahertz spectrometers are expected to provide high performance breath analysis to monitor blood glucose level, metabolism, etc. [8], and a CMOS THz spectrometer is an important step towards low-cost breath analyzers.

In the mid- and high-THz regimes, EM waves can resonate with the vibration modes of biological molecules, which are due to their weak internal connections (such as hydrogen bonds). This is of particular interests since many bio-chemical reactions and structures (e.g. DNA and RNA) are closely related to the hydrogen bonds of molecules [9]. At present, the weak radiated power remains as one of the largest hurdles in building mid-THz spectrometers on chip, because the frequency is already a few times higher than the cutoff frequency of silicon transistors. At present, quasi-optical combination of many coherent radiator units remains a promising solution to the problem, but that requires high-scalability 2D array architecture and compact harmonic radiator structure. To this end, in [3], as many as 91 dipole slot antennas driven by 42 mutually-coupled radiators at 1 THz are implemented in a 130-nm SiGe BiCMOS chip. With the aforementioned versatile electromagnetic structure design [7], this large-scale radiator array achieves $\lambda_{1THz}/2$ optimal antenna pitch (i.e. $\sim 0.1 \times 0.1$ mm² area for each unit), and in total occupies only 1-mm² die size. Its measured total radiated power of 0.1 mW is the highest among all mid-THz sources in

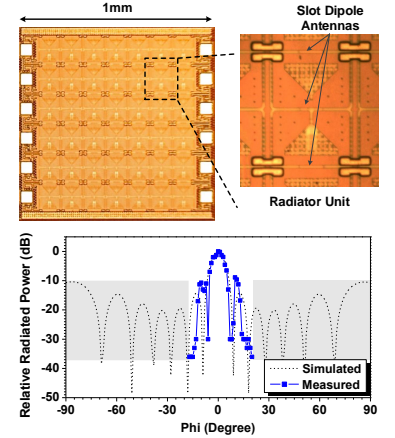


Fig. 3: 1-THz source in SiGe with 91 coherent antennas, and its measured radiation pattern [3].

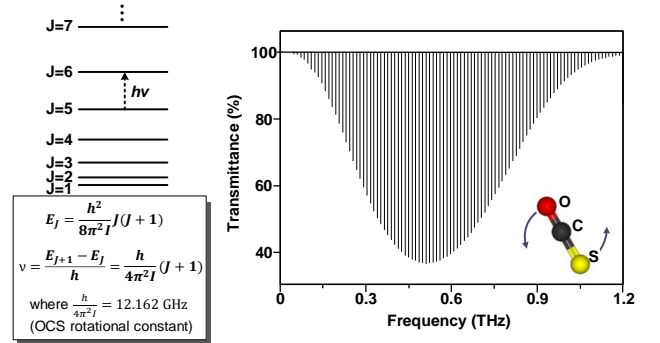


Fig. 4: Quantized rotational energy of OCS and absorption intensity of the transition lines [4].

silicon. It is also noteworthy that its output beam is collimated by $\sim 250\times$, leading to a high equivalent isotropically radiated power (EIRP) of 20 mW.

III. CMOS MOLECULAR CLOCK

A clock reference, which keeps its frequency stability over a long time and under environmental change, is critical for navigation, telecommunication and sensing. It is particularly important when the GPS signal is unavailable (e.g. in underwater, underground and indoor conditions). Unfortunately, the widely adopted crystal oscillators only offer *ppm*-level stability. Chip-scale atomic clocks (CSACs), although offer 10^{-11} -level long stability, are very costly ($> \$1k$) due to their complicated electro-optical construction.

We have demonstrated that the rotational transition lines of linear molecules can be used as stable frequency reference for clocks (hence “molecular clocks”) [4]. In specific, carbonyl sulfide (¹⁶O¹²C³²S) is studied and used. The distribution of rotational energy for OCS (as well as other linear polar molecules) follow a quadratic fashion; this then leads to equally-spaced ($\Delta f_{OCS} \approx 12.162$ GHz) absorption lines [10]. Shown in Fig. 4, the absorption intensity increases

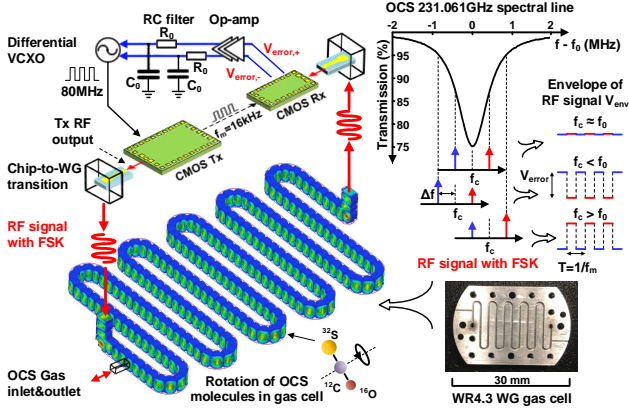


Fig. 5: Diagram of the molecular clock and the spectral-line probing scheme using wavelength modulation and lock-in detection [5].

significantly from RF to low-THz frequency, due to more degenerated sub-levels. As a result, probing a transition line at low-THz frequency not only provide large spectroscopic SNR (hence better short-term clock stability), but also a smaller single-mode-waveguide gas cell. Based on an OCS transition line at 267.530 GHz ($Q=4.7 \times 10^5$), a lab-scale clock prototype using THz transceivers from Virginia Diode Inc. has been demonstrated with a measured Allan deviation of 2.2×10^{-11} ($\tau=1000$ s) [4], which is comparable to that of CSAC's, and orders of magnitude better than crystal oscillators.

What makes the molecular clock attractive is its fully-electronic nature and the potential low-cost implementation using standard CMOS technology. In order to showcase such advantages, the first chip-scale proof-of-concept is demonstrated using a bulk 65-nm CMOS process [5]. It probes an OCS line at $f_0=231.061$ GHz and consumes only 66 mW of DC power (half of that of a CSAC). Shown in Fig. 5, a CMOS transmitter chip, equipped with a 40-bit Σ - Δ PLL, generates a 0.1-mW, wavelength-modulated signal that periodically probes the two slopes of the spectral line. The amplitude and phase of the absorption fluctuation v_{error} , as a result, represent the offset between the probing frequency f_c and the line center. Such information is then used to regulate a 80-MHz voltage-controlled crystal oscillator (VCXO) which feeds the transmitter PLL. The control loop reaches steady state when $v_{error}=0$ and $f_c=f_0$. In the measurement, the Allan deviation of this chip-scale molecular clock reaches 3.8×10^{-10} ($\tau=1000$ s). A more straightforward comparison with a free-running crystal oscillator at 80 MHz is shown in Fig. 6. We see that the molecular clock better stabilizes its frequency over a long period. If large temperature variation occurs, the difference will be even more significant.

With an improved gas cell design, especially more efficient chip-to-waveguide couplers, the chip-scale molecular clock is expected to achieve similar performance as what the lab-scale prototype demonstrated. It is envisioned that such on-chip "atomic clocks" will be widely deployed in future portable navigators, communicators, and networked sensors.

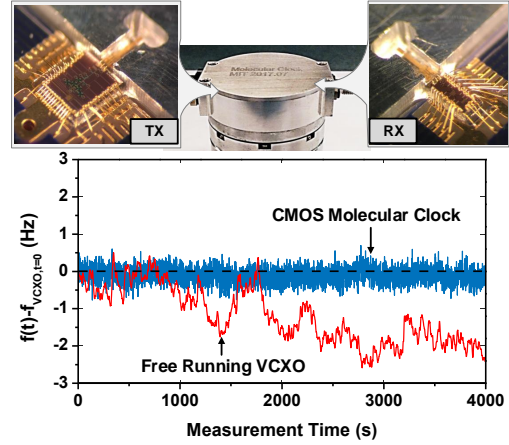


Fig. 6: Prototype of chip-scale molecular clock and the measured instantaneous frequency over 4000 s [4], [5].

IV. ROOM-TEMPERATURE QUANTUM MAGNETOMETER

In the recent years, CMOS circuits are rapidly making their way to the implementation of large-scale quantum computers. Operating at Kelvin-level temperature, they mainly serve as the mixed-mode signal interface between the qubits at a few tens of mK and external electronics at room temperature [11]. In another word, in these systems, CMOS chips, although of great importance, are not directly involved in the physical interactions with the quantum states.

It is noteworthy that quantum systems does not facilitate computation only, it also has extensive applications regarding the sensing of various physical quantities. Unlike quantum computing, where cryogenic condition is needed for long coherence time, quantum sensing can be performed under room temperature. In collaboration with the Quantum Photonics Laboratories at MIT, led by Prof. Dirk Englund, we recently demonstrated the feasibility of room-temperature quantum magnetometry on a CMOS chip [6]. Here, nitrogen vacancy (NV) centers in diamond are used as solid-state quantum sites. Shown in Fig. 7(a), the NV has a ground state spin triplet ($|0\rangle, |\pm 1\rangle$); with the absence of an external field B_z in the N-V axial direction, a microwave at ~ 2.87 GHz causes the transition from $|0\rangle$ to $|\pm 1\rangle$. To detect that transition, a green light ($\lambda=532$ nm) is applied to the diamond, which further moves the NV's to the excited state (3A in Fig. 7(a)). For the NV's with $|0\rangle$ state, fluorescence occurs when they directly transition back to the ground state and red light photons are emitted; for those with $|\pm 1\rangle$ state, a non-radiative decay (hence low fluorescence) occurs due to their transition into a metastable singlet subspace (1A in Fig. 7(a)). Thus, with a sweeping microwave frequency, a dip in the fluorescence response, also called optically-detected magnetic resonance (ODMR) plot, is observed. Now, when a non-zero field B_z is applied, a Zeeman splitting of the $|\pm 1\rangle$ states occurs, leading to two dips in the ODMR plot with a spacing of $\Delta f=2\gamma_e B_z$ ($\gamma_e=2.8$ MHz/Gauss). The value of B_z is therefore derived from a measurement of Δf .

Traditionally, the ODMR plots are measured using a set

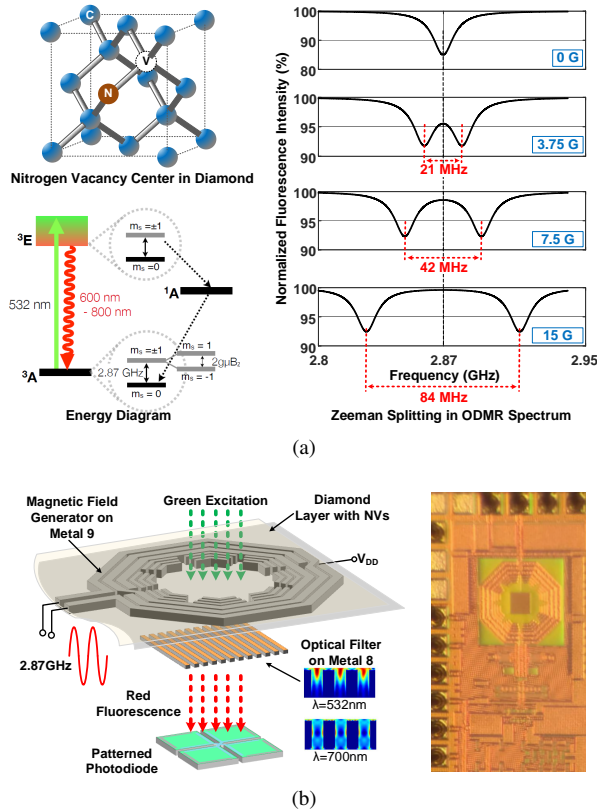


Fig. 7: Magnetometry through quantum sensing on a CMOS chip (a work in collaboration with Prof. Dirk Englund’s group at MIT) [6]: (a) structure and energy diagram of NV centers in diamond, as well as their Zeeman effects. (b) A CMOS magnetometer based on the optically-detected magnetic resonance (ODMR) of the NV centers.

of discrete instruments that are very bulky. In [6], all key components other than the green light source are integrated in a 65-nm CMOS chip. Shown in Fig. 7(b), a layer of nano-diamonds containing NV center ensembles is deposited on the surface of the chip. A multi-loop inductor with its resonance frequency tuned at 2.87 GHz is used to launch ~ 10 Gauss of microwave field at the NV centers. Inside the inductor coil, a capacitively-coupled parasitic loop is added, in order to increase the uniformity of magnetic field (to $\sim 95\%$). This enhances the spin coherence among the NV centers in future pulse-sequence-based experiments, which may lead to ultra-high sensitivity. To detect the red fluorescence from the NV centers, a p+/N-well/p-sub photodiode is placed under the inductor. Due to the high conductivity of the photodiode layer, any eddy current induced by the inductor would decrease the quality factor of inductor. To mitigate this problem, the photodiode and its metal contacts are partitioned so that all large eddy current loop paths are broken. Similar approaches are also used previously in the patterned ground shields of on-chip inductors [12]. Lastly, an on-chip photonic filter is implemented above the photodiode, so that the injected green light, which causes excessive shot noise in the photodiode, is suppressed. This is achieved via a periodic grating structure in the CMOS back-end metal layer, which couples the incident

green light to a lossy surface plasmon polariton mode. With a metal spacing of 400 nm, the filter provides ~ 10 -dB green light suppression. In the experiments, ODMR plots with magnetic-induced splitting are obtained, leading to a sensitivity of $73 \mu\text{T}/\sqrt{\text{Hz}}$. To the author’s best knowledge, this is the first demonstration of CMOS-integrated quantum sensing.

V. CONCLUSION

Through the generation and/or detection of RF-to-optical waves, microchips using standard CMOS/BiCMOS process can perform direct physical interactions with molecules, atoms and electrons. New paradigms of circuit design for material detection, time-keeping, EM sensing and so on are being opened up.

ACKNOWLEDGMENT

All the co-authors of the papers reported here are acknowledged. The spectrometer and clock projects are funded by National Science Foundation (CAREER ECCS-1653100 and ECCS-1809917), MIT Lincoln Laboratories (ACC-672), TDK USA, Texas Instruments, and Singapore-MIT Alliance for Research and Technology.

REFERENCES

- [1] C. Wang and R. Han, “Rapid and Energy-Efficient Molecular Sensing Using Dual mm-Wave Combs in 65nm CMOS: A 220-to-320GHz Spectrometer with 5.2mW Radiated Power and 14.6-to-19.5dB Noise Figure,” in *International Solid-State Circuit Conference (ISSCC)*, San Francisco, CA, 2017, pp. 18–20.
- [2] —, “Molecular Detection for Unconcentrated Gas with ppm Sensitivity Using Dual-THz-Comb Spectrometer in CMOS,” *IEEE Trans. Biomedical Circuits and Systems*, vol. 12, no. 3, pp. 709–721, 2018.
- [3] Z. Hu *et al.*, “High-Power Radiation at 1-THz in Silicon : A Fully Scalable Array Using A Multi-Functional Radiating Mesh Structure,” *IEEE Journal of Solid-State Circuits (JSSC)*, vol. 53, no. 5, pp. 1313–1327, 2018.
- [4] C. Wang *et al.*, “An On-Chip Fully-Electronic Molecular Clock Based on sub-THz Rotational Spectroscopy,” *Nature Electronics*, vol. 1, no. 7, 2018.
- [5] —, “A CMOS Molecular Clock Probing 231.061-GHz Rotational Line of OCS with Sub-ppb Long-Term Stability and 66-mW DC Power,” in *Symposia on VLSI Technology and Circuits*, Honolulu, HI, 2018.
- [6] M. I. Ibrahim *et al.*, “Room-Temperature Quantum Sensing in CMOS : On-Chip Detection of Electronic Spin States in Diamond Color Centers for Magnetometry,” in *Symposia on VLSI Technology and Circuits*, Honolulu, HI, 2018.
- [7] C. Wang *et al.*, “Large-Scale Terahertz Active Arrays in Silicon Using Highly-Versatile Electromagnetic Structures (Invited),” in *IEEE International Electron Device Meeting (IEDM)*, San Francisco, CA, 2017.
- [8] C. F. Neese *et al.*, “Compact submillimeter/terahertz gas sensor with efficient gas collection, preconcentration, and ppt sensitivity,” *IEEE Sensors Journal*, vol. 12, no. 8, pp. 2565–2574, 2012.
- [9] T. Globus *et al.*, “Sub-terahertz vibrational spectroscopy for microRNA based diagnostic of ovarian cancer,” *Convergent Science Physical Oncology*, vol. 2, no. 4, p. 045001, 2016.
- [10] C. H. Townes and A. L. Schawlow, *Microwave Spectroscopy (Dover Books on Physics)*, 2nd ed., 2012.
- [11] B. Patra *et al.*, “Cryo-CMOS Circuits and Systems for Quantum Computing Applications,” *IEEE Journal of Solid-State Circuits*, vol. 53, no. 1, pp. 1–13, 2017.
- [12] C. P. Yue and S. S. Wong, “On-Chip Spiral Inductors with Patterned Ground Shields for Si-Based RF ICs,” *IEEE Journal of Solid-State Circuits (JSSC)*, vol. 33, no. 5, pp. 743–752, 1998.